

Vibrational relaxation of CO by collisions with ^4He at ultracold temperatures

N. Balakrishnan and A. Dalgarno

Institute for Theoretical Atomic and Molecular Physics, Harvard-Smithsonian Center for Astrophysics,
60 Garden Street, Cambridge, Massachusetts 02138

R. C. Forrey

Penn State University, Berks-Lehigh Valley College, Reading, Pennsylvania 19610

(Received 18 February 2000; accepted 13 April 2000)

Quantum mechanical coupled channel scattering calculations are performed for the ro-vibrational relaxation of CO in collisions with ultracold He atoms. The van der Waals well in the interaction potential supports a number of shape resonances which significantly influence the relaxation cross sections at energies less than the well depth. Feshbach resonances are also found to occur near channel thresholds corresponding to the $j=1$ rotational level in the $v=0$ and $v=1$ vibrational levels. Their existence influences dramatically the limiting values of the elastic scattering cross sections and the rotational quenching rate coefficients from the $j=1$ level. We present complex scattering lengths for several low lying rotational levels of CO which characterize both elastic and inelastic collisions in the limit of zero temperature. Our results for the vibrational relaxation of CO ($v=1$) are in good agreement with available experimental and theoretical results. © 2000 American Institute of Physics. [S0021-9606(00)01526-9]

I. INTRODUCTION

The possibility of creating coherent sources of molecular condensates similar to those of atomic Bose-Einstein condensates has generated much interest in low energy atomic and molecular collisions. Several review papers have appeared recently.^{1–4} A major problem that confronts experimental efforts to cool and trap molecules is collisional quenching of ro-vibrational levels leading to trap loss. To help design a stable source of molecular condensates, the efficiency of rotational and vibrational transitions in molecules at ultracold temperatures needs to be investigated.

Techniques based on photoassociation spectroscopy mostly employ ultracold alkali metal atoms as precursors.^{5–8} They produce translationally cold molecules in highly excited vibrational levels. In contrast, the buffer gas loading technique of Doyle and co-workers^{9,10} which is applicable to any paramagnetic molecule employs a buffer gas of ^3He to cool the molecules to a temperature of about 250 mK in a magnetic trap. A method to slow down neutral polar molecules using a time-varying electric field (Stark decelerator) has also been proposed^{11,12} and applied by Meijer and co-workers¹¹ to slow down metastable CO molecules.

Regardless of the specific experimental scheme, the efficiency of cooling depends on the relative magnitude of the elastic and inelastic scattering cross sections. Elastic scattering involves momentum transfer collisions between the buffer gas and the molecules with no changes in internal quantum states. Inelastic atom-molecule collisions involve changes in ro-vibrational energy levels of the molecule and the energy released may be orders of magnitude larger than the typical depth of the traps which is about 1 K. Hence inelastic collisions generally lead to trap loss. Theoretical studies of elastic and inelastic scattering at ultracold temperatures have become crucial in addressing many issues re-

lated to the experiments and also in identifying systems which may be potential candidates for future experiments. Several applications of ultracold molecules have been suggested which include molecular spectroscopy with unprecedented resolution, coherent sources of molecular beams, and the determination of more accurate intermolecular potentials.

We have explored several aspects of ro-vibrational energy transfer collisions at ultracold temperatures^{13–18} by carrying out calculations on the benchmark systems $\text{H}+\text{H}_2$ and $\text{He}+\text{H}_2$. The studies showed that ro-vibrational energy transfer can be extremely efficient at ultracold temperatures and that it is sensitive to the initial ro-vibrational energy levels. It was shown that^{13,15} the energy transfer cross sections obey threshold laws in the limit of zero collision energy. This property was used to construct a complex scattering length for inelastic collisions in which the imaginary part of the scattering length was related to the zero-temperature value of the inelastic quenching rate coefficient. With the aid of the complex scattering length, a kinetic model was constructed¹⁷ for describing the decay of trapped molecules in an ultracold sample taking into account both collisional quenching and vibrational (and rotational) predissociation. It was shown that^{15,16} timescales for vibrational and rotational predissociation can be extracted from the complex scattering length. The calculations so far have focused on homonuclear diatoms. Here we investigate the energy transfer in a heteronuclear system taking $\text{He}+\text{CO}$ as an example.

The He–CO system has been the subject of a large number of experimental and theoretical investigations^{19,21–29} especially in determining the vibrational relaxation efficiency in mixtures of He and CO. Recently, Reid *et al.*^{21,26,27} have published a number of papers addressing the anomalous behavior of the rate coefficient for vibrational relaxation of

$\text{CO}(v=1)$ by collisions with both ^3He and ^4He . They found that the rate coefficients exhibited an upward turn at temperatures of the order of the well depth of the van der Waals interaction potential between He and CO. This was attributed to a series of scattering resonances that were seen in the energy dependent cross section at energies less than the well depth. There are significant discrepancies between their measured and calculated rate coefficients at temperatures comparable to the van der Waals well depth which is approximately 30 K for He–CO.

We consider the vibrational relaxation of CO by collisions with ^4He at ultracold and low temperatures. With a coupled channel scattering formulation, we obtained rate coefficients in better agreement with the measured values at low temperatures than the coupled-states calculation of Reid *et al.*^{26,27} though our results approach those of Reid *et al.* as the temperature is increased.

The paper is organized as follows: In Sec. II we briefly describe the methodology. The results and discussions are given in Sec. III and a summary and conclusions in Sec. IV.

II. METHOD

The quantum mechanical scattering calculations were carried out using the nonreactive scattering program MOLSCAT³⁰ suitably adapted to the present system. We adopted the He–CO interaction potential of Heijmen *et al.*²⁵ because it includes the variation of the interaction potential with respect to the stretching of the CO bond. It is also considered to be superior to the other potentials^{19,23,24} that are available for this system especially in reproducing the bound state energies of the He–CO complex. The potential has a van der Waals minimum of -23.734 cm^{-1} at a separation of 3.46 Å between He and the center of mass of CO with a skew angle of 48.4° and with the CO bond length fixed at its equilibrium value of $r_e = 1.128 \text{ \AA}$. The scattering calculations were carried out by expanding the angular dependence of the potential in Legendre polynomials retaining terms of all orders up to 14. The results were found to be insensitive to additional terms in the expansion. A 15-point Gauss–Legendre quadrature was used to project out the expansion coefficients. For the CO molecule, we used an extended Rydberg potential³¹ $V_{\text{CO}}(r) = -D_e [1 + \sum_{i=1}^3 a_i \rho^i] \times \exp(-a_1 \rho)$ with the parameters $a_i = 3.897 \text{ \AA}^{-1}$, 2.305 \AA^{-2} , and 1.898 \AA^{-3} for $i = 1 - 3$, respectively, where the dissociation energy D_e is taken to be 11.226 eV and $\rho = r - r_e$ is the displacement from the equilibrium bond distance. The vibrational wave functions of the CO molecule were computed in a basis set of Hermite polynomials. A 10 point Gauss–Hermite quadrature was employed to evaluate the matrix elements of the potential between the vibrational wave functions.

Due to the large number of closely spaced rotational levels of the CO molecule, the construction of an appropriate rotor basis set was important in making the calculations affordable. We included rotational levels $j = 0 - 25$ in the $v = 0$ and $v = 1$ vibrational levels. There are seven additional rotational levels in the $v = 0$ level below the $v = 1$ threshold. Their inclusion in the scattering calculation did not influence the results at the energies investigated here. With these basis sets, we believe the cross sections presented here are converged to within 5%.

The coupled-channel Schrödinger equations were solved using the R -matrix method.³² The cross sections for transitions from an initial vibrational–rotational level labeled by quantum numbers vj to a final level labeled by quantum numbers $v'j'$ can be expressed in terms of the corresponding S -matrix elements^{33,34}

$$\begin{aligned} \sigma_{vj \rightarrow v'j'}(E_{vj}) &= \frac{\pi}{(2j+1)k_{vj}^2} \sum_{J=0}^{\infty} (2J+1) \\ &\times \sum_{l=|J-j|}^{|J+j|} \sum_{l'=|J-j'|}^{|J+j'|} |\delta_{jj'} \delta_{ll'} \delta_{vv'} - S_{jj' ll' vv'}^J|^2, \end{aligned} \quad (1)$$

where J and l are, respectively, the total and the orbital angular momentum quantum numbers. The primed quantities denote their unprimed counterparts after the collision. The wave vector for the incoming channel is defined as $k_{vj} = \sqrt{2\mu(E - \epsilon_{vj})/\hbar}$ where E is the total energy, ϵ_{vj} is the eigen energy of the initial ro-vibrational state and μ is the three-body reduced mass. The kinetic energy in the initial channel is given by $E_{vj} = \hbar^2 k_{vj}^2 / (2\mu)$.

The total de-excitation (quenching) cross section from a given initial state is given by

$$\sigma_{vj}^{\text{in}}(E_{vj}) = \sum_{v'j'} \sigma_{vj \rightarrow v'j'}(E_{vj}), \quad (2)$$

where the summation includes both vibrationally inelastic and pure rotationally inelastic transitions but excludes purely elastic $v'j' = vj$ transitions. The quenching rate coefficients are obtained by averaging the cross sections over a Boltzmann distribution of velocities of the incoming atom at a specified temperature T :

$$\begin{aligned} r_{vj}(T) &= (8k_B T / \pi \mu)^{1/2} \frac{1}{(k_B T)^2} \int_0^{\infty} \sigma_{vj}^{\text{in}}(E_{vj}) \\ &\times \exp(-E_{vj}/k_B T) E_{vj} dE_{vj}, \end{aligned} \quad (3)$$

where k_B is the Boltzmann constant.

Vibrational relaxation rate coefficients averaged over a thermal population of rotational levels in the initial vibrational level are given by

$$r_v(T) = \frac{\sum_j (2j+1) \exp[-(\epsilon_{vj} - \epsilon_{v0})/k_B T] \sum_{v' < v, j'} r_{vj \rightarrow v'j'}(T)}{\sum_j (2j+1) \exp[-(\epsilon_{vj} - \epsilon_{v0})/k_B T]}, \quad (4)$$

where the state-to-state rate coefficients $r_{vj \rightarrow v'j'}(T)$ are obtained by replacing $\sigma_{vj}^{\text{in}}(E_{vj})$ by $\sigma_{vj \rightarrow v'j'}(E_{vj})$ in Eq. (3), and the summation over j includes all the occupied rotational levels.

In the limit of zero kinetic energy, it is convenient to express the scattering cross section in terms the scattering length. The scattering length is real for single channel scattering where purely elastic scattering occurs but it has an imaginary part when two or more channels are open due to the presence of inelastic scattering. The complex scattering length may be written $a_{vj} = \alpha_{vj} - i\beta_{vj} = -\lim_{k_{vj} \rightarrow 0} (S_{vj,vj} - 1)/2ik_{vj}$, where α_{vj} and β_{vj} are the real and imaginary parts of the scattering length and $S_{vj,vj}$ is an element of the S matrix corresponding to the initial channel.

The elastic cross section becomes finite in the zero energy limit and its magnitude is given by

$$\sigma_{vj \rightarrow vj}(E_{vj} \rightarrow 0) = 4\pi(\alpha_{vj}^2 + \beta_{vj}^2). \quad (5)$$

In the limit of zero temperature, Wigner's law³⁵ holds and the quenching rate coefficients attain finite values. The imaginary part β_{vj} of the scattering length is related to the total inelastic quenching cross section σ_{vj}^{in} in the limit of zero velocity:¹⁴

$$\beta_{vj} = \lim_{k_{vj} \rightarrow 0} \frac{k_{vj}\sigma_{vj}^{\text{in}}}{4\pi} \quad (6)$$

and the zero temperature quenching rate coefficient is given by^{14,15}

$$r_{vj}(T \rightarrow 0) = 4\pi\beta_{vj}\hbar/\mu. \quad (7)$$

The predissociation lifetime of any Feshbach resonance formed during the collision can be obtained from the complex scattering length according to¹⁴

$$\tau_{vj} = \mu|\alpha_{vj}|^4/(2\hbar\alpha_{vj}\beta_{vj}) = \frac{\sigma_{vj \rightarrow vj}(E_{vj} \rightarrow 0)|\alpha_{vj}|^2}{2r_{vj}(T \rightarrow 0)\alpha_{vj}}. \quad (8)$$

Hence the lifetime is given in terms of the ratio between the limiting values of the elastic cross section and the inelastic quenching rate coefficient. The predissociation linewidth $\Gamma_{vj} = \hbar/\tau_{vj}$.

III. RESULTS AND DISCUSSION

Cross sections for elastic scattering and rotationally and vibrationally inelastic scattering are computed as functions of the center of mass kinetic energy in the range 10^{-5} – 1050.0 cm^{-1} . At the lowest energy, only s -wave scattering occurs in the incident channel. Higher angular momentum partial waves are included for $E_{vj} \geq 10^{-3} \text{ cm}^{-1}$ with $J=0-1$ for $0.001 \leq E_{vj} < 0.01 \text{ cm}^{-1}$, $J=0-6$ for $0.01 \leq E_{vj} < 1.0 \text{ cm}^{-1}$, $J=0-10$ for $1.0 \leq E_{vj} \leq 10.0 \text{ cm}^{-1}$, $J=0-24$ for $10.0 < E_{vj} \leq 100.0 \text{ cm}^{-1}$, and $J=0-40$ for $100.0 < E_{vj} \leq 1050.0 \text{ cm}^{-1}$ to secure convergence of the cross sections in Eq. (1).

At incident energies below the van der Waals well depth the cross sections exhibit oscillations as a function of the kinetic energy that are characteristic of resonances. The nature of the oscillations and their role in determining the low temperature rate coefficients have been the subject of several

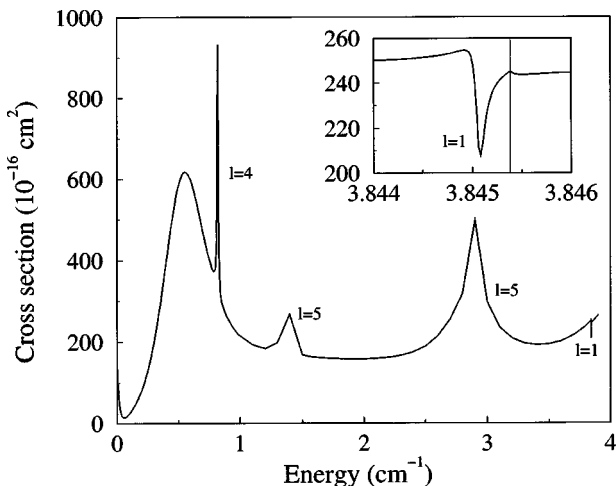


FIG. 1. Elastic scattering cross section in the $v=0, j=0$ level of CO in collisions with ${}^4\text{He}$ as a function of the kinetic energy. The resonances are labeled by the corresponding partial waves. The inset shows a Feshbach resonance in the vicinity of the opening of the $v=0, j=1$ level. The vertical line in the inset corresponds to the $j=1$ threshold.

recent investigations by Reid *et al.*^{21,22,26,27} who identified a number of shape resonances in the energy range of 0.1 – 15 cm^{-1} . We find that both shape resonances and Feshbach resonances occur and that the presence of Feshbach resonances greatly influences the low energy scattering cross sections. In Fig. 1 we show the elastic scattering cross section in the $v=0, j=0$ channel near the opening of the $v=0, j=1$ level. The different angular momentum partial waves contributing to the resonances are labeled in the figure. The $l=4$ and the $l=5$ resonances are shape resonances whereas the narrow $l=1$ resonance is a Feshbach resonance. The inset shows a magnified view of the Feshbach resonance. The cross section varies by about 40 \AA^2 in the narrow energy range of the Feshbach resonance and it exhibits a cusp exactly at the $v=0, j=1$ threshold marked by the vertical line in the inset. This is the Wigner cusp, which occurs at the opening of a channel.

The presence of the Feshbach resonance shown in Fig. 1 has dramatic consequences on the elastic and inelastic scattering in the $v=0, j=1$ channel as the kinetic energy approaches zero. In Fig. 2 we compare the elastic scattering cross sections in the $j=0$ and $j=1$ levels in $v=0$ as functions of the center of mass kinetic energy. Due to the presence of the Feshbach resonance, the limiting value of the elastic cross section in the $j=1$ channel is three orders of magnitude larger than that in the $j=0$ level. The rotational quenching cross section of the $j=1$ level and the corresponding rate coefficient are shown in Fig. 3 and they also assume large values in the limit of zero velocity due to the Feshbach resonance. The quenching rate coefficient is finite in the limit $T \rightarrow 0$ because the corresponding cross section varies inversely as the velocity. The zero temperature quenching rate coefficient is $2.4 \times 10^{-10} \text{ cm}^3 \text{ s}^{-1}$ which is of the order of gas kinetic values.

A similar Feshbach resonance is found to exist below the $v=1, j=1$ threshold as shown in Fig. 4 where we plot the elastic scattering cross section in the $v=1, j=0$ channel in

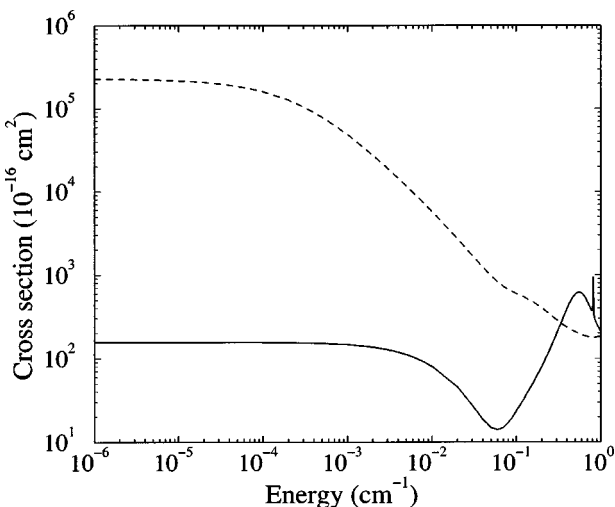


FIG. 2. Comparison of the elastic scattering cross section in the $v = 0, j = 0$ (full curve) and $v = 0, j = 1$ (dashed curve) levels of CO in collisions with ${}^4\text{He}$ as a function of the kinetic energy. The enhancement by three orders of magnitude for the limiting value of the cross section in the $j = 1$ level is due to the Feshbach resonance shown in Fig. 1.

the vicinity of the $v = 1, j = 1$ threshold. The effect of this Feshbach resonance on the low energy quenching cross section from the $v = 1, j = 1$ level will be discussed below.

The vibrational quenching cross sections are very small compared to pure rotational quenching cross sections. This is due to the weak dependence of the interaction potential with respect to the stretching of the CO bond compared to the angular anisotropy. Figure 5 shows the quenching cross section given by Eq. (2) for the $v = 1, j = 0$ level as a function of the relative translational energy. The narrow oscillations that are seen in the energy range $E_{vj} = 0.1 - 10.0 \text{ cm}^{-1}$ are due to shape resonances supported by the van der Waals interaction potential. In the limit of zero energy, only the s -wave contributes and the cross section approaches the inverse velocity

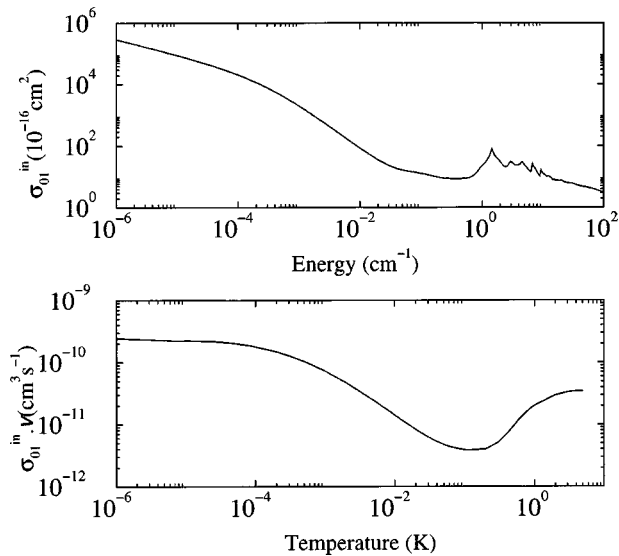


FIG. 3. Upper panel: cross section for quenching of the $v = 0, j = 1$ level of CO in collisions with ${}^4\text{He}$ as a function of the kinetic energy. Lower panel: Corresponding rate coefficient as a function of the temperature.

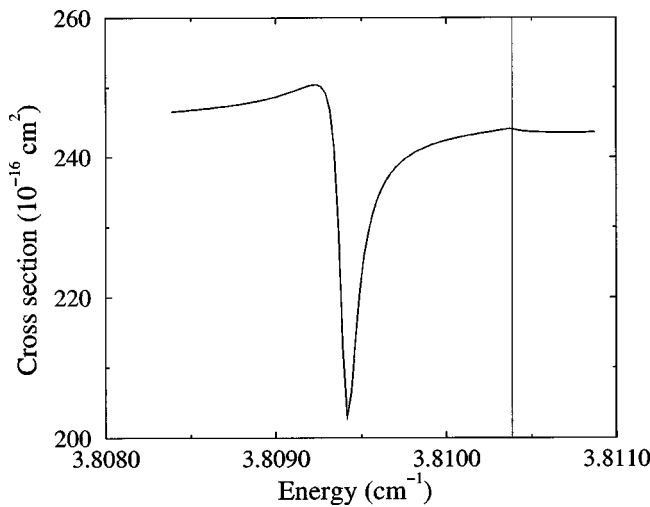


FIG. 4. Feshbach resonance in the elastic scattering cross section in the $v = 1, j = 0$ level below the opening of the $v = 1, j = 1$ level shown by the vertical line. The energy is relative to the $v = 1, j = 0$ level.

dependence of Wigner's law. In Table I we compare our results with those obtained by Reid *et al.*²⁶ at energies between 5.0 cm^{-1} and 1050.0 cm^{-1} . Reid *et al.* used the same interaction potential employed in this study but adopted a coupled-states formalism for the scattering calculations. The discrepancy is never more than a factor of 2 and lessens with increase in energy.

Reid *et al.*²⁶ have presented graphically $v = 1$ quenching rate coefficients by ${}^4\text{He}$ down to a temperature of 10 K. The figure shows a rate coefficient decreasing monotonically down to a value of about $1.0 \times 10^{-20} \text{ cm}^3 \text{ s}^{-1}$. In Fig. 6 we show the quenching rate coefficient given by Eq. (3) for the $v = 1, j = 0$ and $v = 1, j = 1$ levels as functions of the temperature in the range 10^{-5} K to 100 K . The temperature dependence and the magnitude of the two rate coefficients are very similar for $T > 30 \text{ K}$ but surprisingly different for $T < 30 \text{ K}$. The value of the rate coefficient is about $2.5 \times 10^{-20} \text{ cm}^3 \text{ s}^{-1}$ at 30 K. With subsequent decrease of tem-

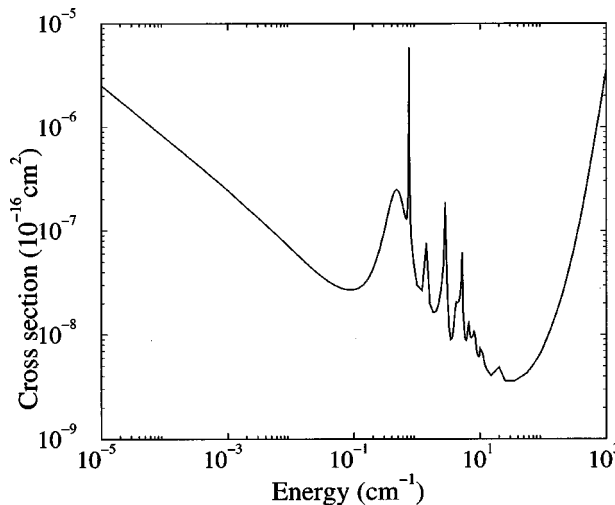


FIG. 5. Cross section for the quenching of the $v = 1, j = 0$ level of CO in collisions with ${}^4\text{He}$ as a function of the kinetic energy.

TABLE I. Comparison between the quenching cross sections from the $v=1, j=0$ level of CO in collisions with ${}^4\text{He}$ obtained in the present close-coupled calculation and the coupled-states calculation of Reid *et al.*

Kinetic energy (cm $^{-1}$)	$\sigma_{10}^{\text{in}} (\text{\AA}^2)$	
	This work	Reid <i>et al.</i> (Ref. 26)
5	0.320×10^{-7}	0.169×10^{-7}
10	0.743×10^{-8}	0.401×10^{-8}
15	0.405×10^{-8}	0.194×10^{-8}
25	0.362×10^{-8}	0.255×10^{-8}
35	0.360×10^{-8}	0.287×10^{-8}
55	0.427×10^{-8}	0.317×10^{-8}
70	0.514×10^{-8}	0.379×10^{-8}
85	0.617×10^{-8}	0.448×10^{-8}
130	0.110×10^{-7}	0.765×10^{-8}
240	0.359×10^{-7}	0.245×10^{-7}
390	0.130×10^{-6}	0.875×10^{-7}
790	0.147×10^{-5}	0.963×10^{-6}
1050	0.444×10^{-5}	0.295×10^{-5}

perature both attain a local minimum near 20 K and rise to a local maximum between 0.7–1.0 K. The $j=0$ rate coefficient drops with further decrease of temperature and eventually attains a limiting value of $6.5 \times 10^{-21} \text{ cm}^3 \text{ s}^{-1}$ for $T < 10^{-3} \text{ K}$. The $j=1$ rate coefficient also drops to a minimum value of $3.4 \times 10^{-20} \text{ cm}^3 \text{ s}^{-1}$ at about 0.3 K but it increases dramatically with further decrease of temperature reaching a limiting value of about $9.0 \times 10^{-19} \text{ cm}^3 \text{ s}^{-1}$ at $T = 10^{-5} \text{ K}$. The initial upturn of the rate coefficients after reaching a minimum value near 20 K is due to the presence of the van der Waals well which accelerates the particles into the interaction zone as the incident kinetic energy falls below the well depth. The resonances in the cross section (shown in Fig. 5 for the $v=1, j=0$ level) make an important contribution to the upturn of the rate coefficients but the limiting value of the rate coefficient is determined purely by the s -wave contribution. The initial fall in the values of the rate coefficients before attaining the zero temperature limit is due to the decay of higher partial waves. The $j=0$ and $j=1$ cases are distinguished by the dramatic rise in the rate coef-

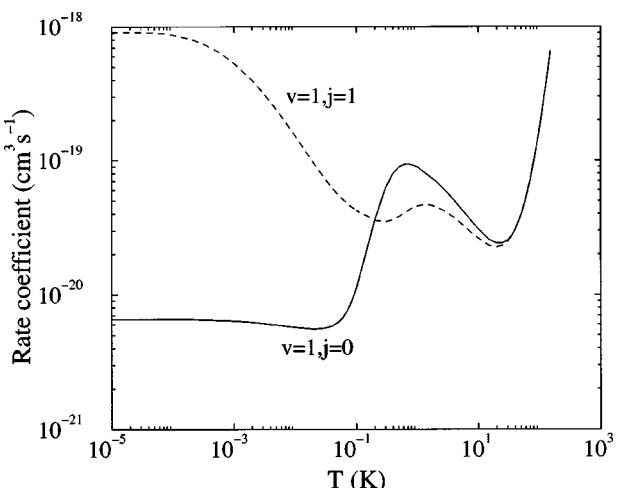


FIG. 6. Rate coefficient for the quenching of the $v=1, j=0$ and $v=1, j=1$ levels of CO in collisions with ${}^4\text{He}$ as functions of the temperature.

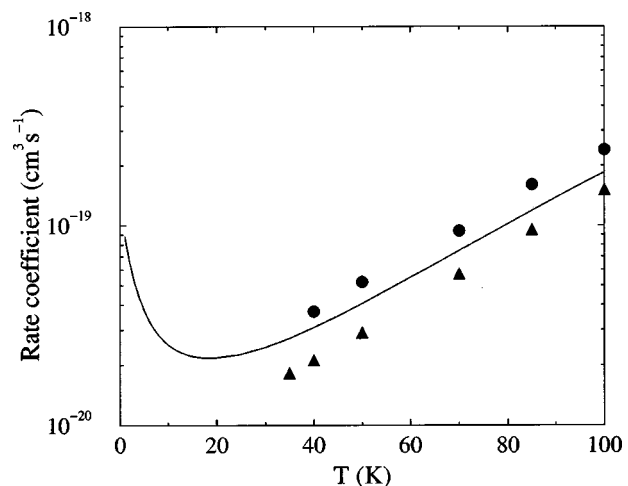


FIG. 7. Rate coefficient for the quenching of the $v=1$ vibrational level of CO in collisions with ${}^4\text{He}$ as a function of the temperature. The experimental data of Wilson *et al.* (Ref. 20) and the theoretical result of Reid *et al.* (Ref. 26) are shown, respectively, by the filled circles and triangles.

ficient below $T=0.3 \text{ K}$ for $j=1$ which is due to the formation of the Feshbach resonance shown in Fig. 4. The Feshbach resonance arises from s -wave scattering in the $v=1, j=1$ level and because it occurs very close to the threshold, it is an example of a *zero energy resonance*.

The rate coefficients for the relaxation of the $v=1$ level has been measured by Wilson *et al.*²⁰ from 40–150 K and Reid *et al.*²⁶ have computed them using cross sections derived from coupled-state calculations. Figure 7 compares our rate coefficients computed using Eq. (4) with the theoretical results of Reid *et al.*²⁶ and the experimental data of Wilson *et al.*²⁰ Our theoretical values are in better agreement with the experimental data. At the lowest temperature of 40 K for which experimental results are available the theoretical prediction nearly coincides with the measurement. The largest deviation from the experimental values is a factor of 1.3 occurring at 100 K. The theoretical predictions are consistently smaller than the experimental values. The difference may be due to an inadequate treatment of the higher rotational levels in $v=1$. We have restricted the sums in Eq. (4) to be $j \leq 3$ to minimize the computational expenses. This is adequate for the lowest temperature where experimental results are available but not at 100 K. The exact behavior of the rate coefficient at temperatures below 40 K has not been determined experimentally and it will be interesting to see if it shows the predicted upward trend. A similar upward trend has been seen in the measured relaxation rate coefficients of CO by H₂ and its isotopomers.²² For these systems, the van der Waals well is deeper at about 60 K for CO–H₂. Hence experimental studies were able to explore the influence of the van der Waals interaction potentials at significantly higher temperatures.

Due to the large number of closely spaced rotational levels of the CO molecule, calculations involving excited vibrational levels of the molecule are prohibitively expensive. Hence we have restricted our calculations to the quenching of the $v=1$ level and a few lowest lying rotational levels in $v=0$. The real and imaginary parts of the

TABLE II. The real and imaginary parts of the scattering length in Å.

v, j	0,0	0,1	0,2	0,3	0,4	0,5	1,0	1,1
α_{vj}	-3.53	127.70	-27.67	-15.23	-9.83	-6.95	-4.32	76.56
β_{vj}	0.0	9.35	16.85	15.40	13.37	11.46	2.90×10^{-10}	2.08

scattering lengths are listed in Table II. The resonance parameters are summarized in Table III. The energy and width of the Feshbach resonances shown in Figs. 1 and 4 calculated from the complex scattering length¹⁴ are in good agreement with those from the close-coupled scattering calculations through the eigenphase sum method.¹⁶

The distribution of rotational levels of CO after collisions with He has been the topic of experimental and theoretical investigations. Antonova *et al.*²⁸ performed measurements of rotational excitation of CO at center of mass collision energies of 72 and 89 meV using crossed molecular beams. The experimental results were modeled by performing close-coupled scattering calculations within the rigid rotor model with results that satisfactorily reproduced the experimental data. Our close-coupled calculations which do not employ the rigid rotor approximation produced cross sections in close agreement with those of Antonova *et al.*²⁸ and are not reproduced here.

In Figs. 8(a), 8(b), and 8(c) we show the distribution of final rotational levels j' following the quenching of the molecule from $v = 1, j = 0, 1$, and 2, respectively, at a center of mass collision energy of 10^{-5} cm^{-1} . The distribution is similar at energies below 10^{-5} cm^{-1} . The cross sections for vibrational transitions are several orders of magnitude smaller than for pure rotational transitions. The rotational distribution shows that a significant fraction of the vibrational energy is converted to rotational energy. The distribution peaks near $j' = 11$ for $j = 0$ and $j' = 8$ for $j = 1$ and 2. The magnitude of the quenching cross sections from $j = 1$ and 2 are, respectively, about 100 and 20 times larger than that from the $j = 0$ level. This is in part due to the strong angular anisotropy of the interaction potential resulting from the dipolar forces which become more important when the molecule is initially oriented. However, the factor of 5 enhancement of the cross section for the $j = 1$ level compared to the $j = 2$ level is due to the presence of the Feshbach resonance shown in Fig. 4.

The distribution of final rotational levels for the above initial states becomes flatter at higher energies. This is illustrated in Figs. 9(a) and 9(b) for the $v = 1, j = 0$ level at center of mass energies of 100 and 500 cm^{-1} , respectively. The nature of the distribution is modified because only s -wave scattering occurs in the incoming channel at 10^{-5} cm^{-1} .

TABLE III. Resonance energies and widths in cm^{-1} and lifetimes in seconds of the $v = 0, j = 1$ and $v = 1, j = 1$ resonances.

v, j	E_{vj}^a	E_{vj}^b	Γ_{vj}^a	Γ_{vj}^b	τ_{vj}^b
0 1	-3.23×10^{-4}	-2.90×10^{-4}	8.0×10^{-5}	8.55×10^{-5}	6.20×10^{-8}
1 1	-9.70×10^{-4}	-8.19×10^{-4}	1.20×10^{-4}	8.90×10^{-5}	5.96×10^{-8}

^aFrom numerically exact close-coupling calculations.

^bFrom scattering length approximation.

whereas a number of higher angular momentum partial waves contribute at higher energies leading to a broader distribution of rotational levels in the outgoing channel.

IV. SUMMARY AND CONCLUSIONS

Explicit quantum mechanical scattering calculations are carried out to investigate the quenching of rotation and vibration of a heteronuclear molecule at ultracold temperatures by taking the He–CO system as an illustrative example. The quenching rate coefficients attain finite values in the limit of zero temperature in accordance with quantum mechanical threshold laws but their magnitude is found to be strongly enhanced by the occurrence of Feshbach resonances. The elastic and inelastic scattering in the limit of zero temperature are characterized by a complex scattering length whose imaginary part is directly related to the zero temperature quenching rate coefficients. Good agreement is obtained with experimental results for the vibrational relaxation $\text{CO}(v = 1)$. It will be interesting to see if the unusual behavior of the low temperature rate coefficients that we predict can be experimentally verified. The Stark decelerator scheme

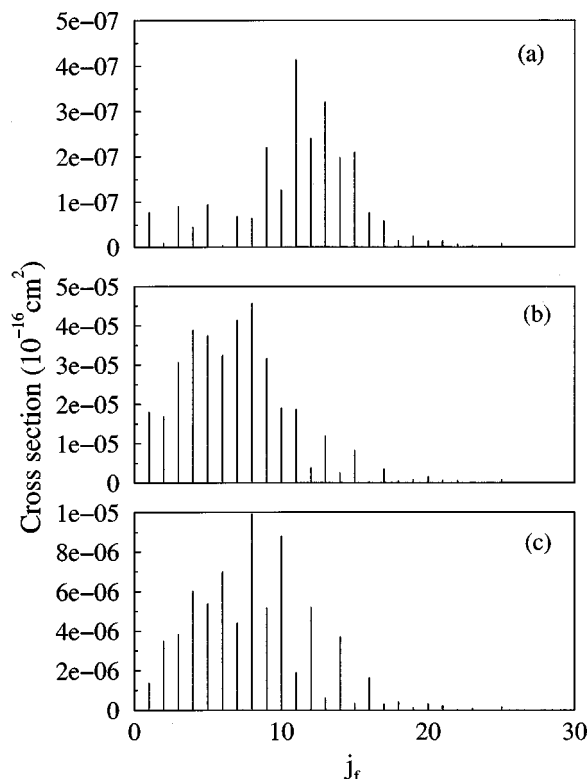


FIG. 8. Distribution of final rotational levels in $v = 0$ following quenching of the $v = 1, j$ levels of CO in collisions with ${}^4\text{He}$ at an incident kinetic energy of 10^{-5} cm^{-1} . The upper panel is for $j = 0$, the middle panel is for $j = 1$ and the bottom panel is for $j = 2$.

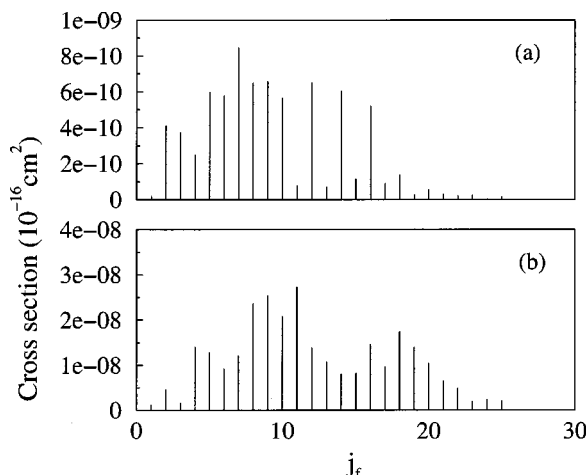


FIG. 9. Distribution of final rotational levels in $v = 0$ following quenching of the $v = 1, j = 0$ level of CO in collisions with ${}^4\text{He}$. The upper panel (a) is for an incident kinetic energy of 100 cm^{-1} and the lower panel (b) is for an incident kinetic energy of 500 cm^{-1} .

of Meijer and co-workers¹¹ has been applied to slow down metastable CO molecules but its applicability is not restricted to metastable species.

ACKNOWLEDGMENTS

This work was supported by the U.S. Department of Energy, Division of Chemical Sciences, Office of Basic Energy Sciences, Office of Energy Research. N.B. is grateful to Professor van der Avoird for providing the He–CO interaction potential.

- ¹J. Weiner, V. S. Bagnato, S. Zillo, and P. S. Julienne, Rev. Mod. Phys. **71**, 1 (1999).
- ²F. Dalfovo, S. Giorgini, L. P. Pitaevskii, and S. Stringari, Rev. Mod. Phys. **71**, 463–512 (1999).
- ³C. E. Wieman, D. E. Pritchard, and D. J. Wineland, Rev. Mod. Phys. **71**, S253–S262 (1999).
- ⁴D. R. Herschbach, Rev. Mod. Phys. **71**, S411 (1999).
- ⁵Y. B. Band and P. S. Julienne, Phys. Rev. A **51**, R4317 (1995).
- ⁶J. T. Bahns, W. C. Stwalley, and P. L. Gould, J. Chem. Phys. **104**, 9689 (1996).
- ⁷R. Côté and A. Dalgarno, Chem. Phys. Lett. **279**, 50 (1997).

- ⁸A. Fioretti *et al.*, Phys. Rev. Lett. **80**, 4402 (1998).
- ⁹J. M. Doyle, B. Friedrich, J. Kim, and D. Patterson, Phys. Rev. A **52**, R2515 (1995).
- ¹⁰J. D. Weinstein *et al.*, Nature (London) **395**, 148 (1998).
- ¹¹H. L. Bethlehem, G. Berden, and G. Meijer, Phys. Rev. Lett. **83**, 1558 (1999).
- ¹²J. A. Maddi, T. P. Dinneen, and H. Gould, Phys. Rev. A **60**, 3882 (1999).
- ¹³N. Balakrishnan, R. C. Forrey, and A. Dalgarno, Chem. Phys. Lett. **280**, 1 (1997).
- ¹⁴N. Balakrishnan, V. Kharchenko, R. C. Forrey, and A. Dalgarno, Chem. Phys. Lett. **280**, 5 (1997).
- ¹⁵N. Balakrishnan, R. C. Forrey, and A. Dalgarno, Phys. Rev. Lett. **80**, 3224 (1998).
- ¹⁶R. C. Forrey, N. Balakrishnan, V. Kharchenko, and A. Dalgarno, Phys. Rev. A **58**, R2645 (1998).
- ¹⁷R. C. Forrey, V. Kharchenko, N. Balakrishnan, and A. Dalgarno, Phys. Rev. A **59**, 2146 (1999).
- ¹⁸R. C. Forrey *et al.*, Phys. Rev. Lett. **82**, 2657 (1999).
- ¹⁹R. J. LeRoy *et al.*, Faraday Discuss. **97**, 81 (1994).
- ²⁰G. J. Wilson, M. L. Turnidge, A. S. Solodukhin, and C. J. S. M. Simpson, Chem. Phys. Lett. **207**, 521 (1993).
- ²¹J. P. Reid, C. J. S. M. Simpson, and H. M. Quiney, Chem. Phys. Lett. **246**, 562 (1995).
- ²²J. P. Reid, C. J. S. M. Simpson, H. M. Quiney, and J. M. Hutson, J. Chem. Phys. **103**, 2528 (1995).
- ²³R. Moszynski, T. Korona, P. E. S. Wormer, and A. van der Avoird, J. Chem. Phys. **103**, 321 (1995).
- ²⁴M. Thachuk, C. E. Chuaqui, and R. J. LeRoy, J. Chem. Phys. **105**, 4005 (1996).
- ²⁵T. G. A. Heijmen, R. Moszynski, P. E. S. Wormer, and A. van der Avoird, J. Chem. Phys. **107**, 9921 (1997).
- ²⁶J. P. Reid, C. J. S. M. Simpson, and H. M. Quiney, J. Chem. Phys. **107**, 9929 (1997).
- ²⁷J. P. Reid and C. J. S. M. Simpson, Chem. Phys. Lett. **280**, 367 (1997).
- ²⁸S. Antonova, A. Lin, A. P. Tsakotellis, and G. C. McBane, J. Chem. Phys. **110**, 2384 (1999).
- ²⁹M. M. Ahern, D. A. Steinhurst, and M. A. Smith, Chem. Phys. Lett. **300**, 681 (1999).
- ³⁰J. M. Hutson and S. Green, MOLSCAT computer code, version 14 (1994), distributed by Collaborative Computational Project No. 6 of the Engineering and Physical Sciences Research Council (UK).
- ³¹J. N. Murrell *et al.*, *Molecular Potential Energy Functions* (Wiley, New York, 1984).
- ³²E. B. Stechel, R. B. Walker, and J. C. Light, J. Chem. Phys. **69**, 3518 (1978).
- ³³A. M. Arthurs and A. Dalgarno, Proc. R. Soc. London, Ser. A **256**, 540 (1963).
- ³⁴W. A. Lester, Jr., in *Dynamics of Molecular Collisions*, Part A, edited by W. H. Miller (Plenum, New York, 1976), pp. 1–32.
- ³⁵E. P. Wigner, Phys. Rev. **73**, 1002 (1948).